Composition Wheels: Visualizing dissolved organic matter using common composition metrics across a variety of Canadian Ecozones

Pieter J. K. Aukes[1,2¶*]

Sherry L. Schiff[1¶]

[1] Department of Earth & Environmental Studies, University of Waterloo, Waterloo, Ontario, Canada

[2] Geography & Environmental Studies, Wilfrid Laurier University, Waterloo, Ontario, Canada

* Corresponding author

E-mail: paukes@uwaterloo.ca (PJKA)

[¶]These authors contributed equally to this work.

Abstract

Dissolved organic matter (DOM) is a ubiquitous component of aquatic systems, impacting aquatic health and drinking water quality. These impacts depend on the mixture of organic molecules that comprise DOM. Changing climates are altering both the amount and character of DOM being transported from the terrestrial system into adjacent surface waters, yet DOM composition is not monitored as often as overall concentration. Many DOM characterization methods exist, confounding comparison of DOM composition across different studies. The objective of this research is to determine which parameters in a suite of relatively simple and common DOM characterization techniques explain the most variability in DOM composition from surface and groundwater sites. Further, we create a simple visualization tool to easily compare compositional differences in DOM. A large number of water samples (n=250) was analyzed from six Canadian ecozones for DOM concentration, ultraviolet-visible light absorbance, molecular size, and elemental ratios. Principal component analyses was used to identify quasi-independent DOM compositional parameters that explained the highest variability in the dataset: spectral slope, specific-UV absorbance at 255nm, humic substances fraction, and dissolved organic carbon to dissolved organic nitrogen ratio. A 'Composition Wheel' was created by plotting these four parameters as a polygon. Our results find similarities in DOM composition irrespective of site differences in vegetation and climate. Further, two main end-member Composition Wheel shapes were revealed that correspond to DOM in organic-rich groundwaters and DOM influenced by photodegradation. The Composition Wheel approach uses easily visualized differences in polygon shape to quantify how DOM evolves by natural processes along the aquatic continuum and to track sources and degradation of DOM.

Introduction

Dissolved organic matter (DOM) is a pervasive component of aquatic environments and an important determinant of overall water quality and ecosystem function. For example, DOM dictates light, thermal, and pH regimes within lakes [1], complexes with and mobilizes metals [2], and acts as an important redox constituent for biogeochemical reactions [3]. Further, DOM affects drinking water quality through taste, odour, and colour [4], consumption of added oxidizing chemicals, and reactions with chlorine during drinking water treatment processes to form carcinogenic disinfection by-products [5]. The overall reactivity of DOM is determined by its mixture of thousands of organic molecules with differing structural and chemical characteristics. Increased DOM concentrations have been observed in surface waters across the

United Kingdom, Europe, and North America [1,6] and linked with declines to water transparency [1,7], that may, in turn have significant effects upon future drinking water treatment options [8,9]. Yet, little information is found on the processes that dictate DOM composition and its impact on the surrounding environment [10]. Hence, quantifying changes to both the amount and composition of DOM across temporal and spatial scales allows for a better understanding of future changes to DOM and its influence upon water quality.

Both concentration and composition of DOM are used to identify the source, quality, and fate of DOM within the environment. The overall DOM concentration is operationally quantified by the concentration of carbon in molecules passing through a chosen filter size (generally between 0.2 and 0.7 μm), whereas DOM composition refers to the mixture of organic molecules that comprise it. Differences in DOM composition have been used to quantify hydrologic mixing and changes to redox potential [11]. Various options are available to characterize DOM composition, but many are expensive, analyze only a subfraction of the DOM, require complicated analysis, or are not widely accessible. For instance, Fourier transform ion cyclotron resonance mass spectrometry (FT-ICR-MS) analyses provides insightful and novel information on DOM composition [12,13] but is not readily available. Alternatively, a number of common and simple measures can provide compositional information on bulk DOM. Ultraviolet and visible light absorbance are used to estimate aromaticity and molecular size of light-absorbing DOM [14–16], while fluorescence provides information on the amount of humic and proteinaceous DOM [17,18]. Simple elemental ratios, such as dissolved organic carbon to dissolved organic nitrogen, indicate DOM lability [19], whereas comparison of various molecular weight groupings can identify differences in DOM sources or processes (i.e. large humic substances from soil-derived sources versus low-molecular weight components from

enhanced degradation) [20]. Thus, various characterization techniques can provide a holistic representation of the components that comprise DOM.

Dissolved organic matter is the net product of varying sources and degrees of processing at a point within the watershed. Quantifying changes to DOM composition along a hydrologic continuum can provide information on dominant sources or processes that influence DOM evolution [21]. For instance, DOM sampled from organic-rich substrates typically has high concentrations of large molecular weight, aromatic DOM, while enhanced processing in groundwaters shifts DOM towards smaller components [22–24]. Soil-derived DOM characteristics dominate in headwater streams across various climatic regimes, as shown by higher UV-absorbing properties and higher molecular weight components [18,21]. Conversely, exposure to sunlight and *in-situ* DOM production within surface waters produces DOM with lower UV-absorbing, low-molecular weight components [15]. Once in the aquatic system, differences in DOM composition, or intrinsic controls, are thought to dictate DOM fate more-so than extrinsic controls such as temperature, nutrients, and sunlight exposure [25]. Soil-derived aliphatic components of DOM are preferentially lost as water moves from subsurface to surface waters, at which point aromatic, high-nominal oxidation state DOM becomes further degraded along the fluvial network to more aliphatic, low nominal oxidation state DOM [12,25]. Increased degradation and processing of DOM along the hydrologic continuum reduces its chemodiversity, with persistence of specific components linked to the original DOM composition [25–27]. Hence, compositional measures can be used to better understand how DOM composition varies, and the potential sources or processes that have resulted in the specific mixture of DOM at that point of sampling.

Recent progress in the understanding of DOM and carbon cycling has led to recognition of the importance of characterizing DOM composition along with concentration. Although characterization techniques have improved [28], the final synthesis and discussion of various compositional DOM measures has generally relied on a matrix of scatter plots, requiring the user to jump between graphs and build the comparison themselves. Given the direct impact of DOM composition on water treatment and aquatic health, there is a need to relay compositional information in an efficient and understandable manner to inform policy decisions. This can be difficult if numerous graphs are needed in order to compare DOM differences, all with units and scales specific to the method, especially if the target audience has little knowledge of carbon chemistry or the characterization techniques.

Clear communication of science and its relevance to society is increasing in importance for both informing the general public and supporting evidence-based policy decisions. Effective data visualization can reduce the cognitive load required to understand and retain new knowledge [29,30], creating an accessibility to science that enhances scientific literacy [31–33]. Recently, scientists and graphic designers have collaborated to utilize large datasets and translate data-driven conclusions using novel, creative techniques [34,35]. In terms of DOM composition, graphics have not moved beyond various scatter plots. Further, comparison of different DOM composition metrics have generally focussed on single hydrological environments (i.e. solely lakes [26] or rivers [36]) or on one or two measures across spatial scales or varying environments. Given the complex mixture of organic compounds, and that different measures of DOM composition record different attributes, the combined use of several complimentary measures may provide a better characterization of DOM [37] and enhance public outreach through presentation as a simple, effective image.

The objectives of this study are to select the best suite of readily accessible DOM characterization techniques, and to create a simple, effective visual tool that can be used to illustrate and discuss differences in DOM composition across environmental gradients. These objectives will be accomplished in three parts: 1) determine which broadly-used measures of DOM composition capture the most variability within a dataset of surface and groundwater sites in various Canadian ecozones (groupings of similar areas of biodiversity [38]), 2) create a visualization tool to allow facile comparison of DOM from different samples based upon a set of quasi-independent composition measures, and 3) use the tool to explore DOM composition resulting from differences in hydrological setting and climate across a range of northern environments.

Methods

Sites & sampling

Locations were selected where DOM was expected to differ due to differences in surrounding watershed characteristics (e.g. land use, wetland coverage, climate, and vegetation). Various surface and groundwater samples were collected between June to October from the Northwest Territories (Yellowknife, Wekweètì, Daring Lake), high arctic Nunavut (Lake Hazen Watershed), and Ontario (IISD-Experimental Lakes Area) (Fig 1; S1 Table). Surface water samples were collected 0.25 m below the surface from lakes, rivers, creeks, and ponds. Groundwater samples from northern locations (Yellowknife, Wekweètì, Daring Lake, Lake Hazen) were collected from the deepest extent of the mid-summer active-layer, just above the permafrost boundary (0.1 to 0.5 m below surface). Additional samples were collected from Turkey Lakes Watershed (ON), Nottawasaga River Watershed (ON), Grand River (ON),

Mackenzie River (NT), and Black Brook Watershed (NB) to expand the ranges of individual composition measures but only overall DOM concentration and select composition metrics are available at these sites (Fig 1; S1 Table). A total of 250 samples were collected and analysed in this study.

Surface water samples were collected using a 60 mL syringe and filtered in-field using 0.45 μm syringe-tip filters (Whatman GD/X 45mm) into 40 mL acid-washed, pre-rinsed glass vials. Groundwater samples were collected using a peristaltic pump with an attached 0.45 μm syringe-tip filter. Vials and filters were pre-rinsed with filtered sample water before collection. Samples were kept cool (<4ºC) and in the dark until analysis at the University of Waterloo within three weeks of collection.

DOM quantity & composition analyses

Dissolved organic carbon and total nitrogen concentrations were measured using a Shimadzu Total Organic Carbon (TOC-L) Combustion Analyzer with TNM-1 module. Dissolved organic nitrogen (DON) was calculated as the difference between total dissolved nitrogen concentration and the sum of inorganic nitrogen species (nitrate, nitrite, and ammonium). Inorganic nitrogen species were measured using SmartChem 200 Automated Chemistry Analyzer (Unity Scientific, MA United States). The DOC:DON ratio was calculated using molar concentrations of DOC (M_C) and DON (M_N).

Absorbance was measured in a 1 cm cuvette using a Cary 100 UV-VIS Spectrophotometer (Agilent, CA United States) at 5 nm increments from 200 to 800 nm. Deionized water was used to zero the instrument and run intermittently during analyses to correct for baseline drift. The Naperian absorption coefficient (a; m^{-1}) was calculated using:

$$a_\lambda = \frac{ln(10) \times A_\lambda}{L}$$

where A is the baseline-corrected absorbance at wavelength λ and L is the cell length (m). A suite of absorbance characteristics were then calculated (Table 1).

Molecular-size based fractions of DOM were determined using a size exclusion chromatography technique (Liquid Chromatography – Organic Carbon Detection, LC-OCD) at the University of Waterloo. Detailed instrument setup and analysis is described elsewhere [20]. Briefly, the sample was injected through a size-exclusion column (SEC; Toyopearl HW-50S, Tosoh Bioscience) that separated DOM based on hydrodynamic radii into five hydrophilic fractions (from largest to smallest): biopolymers (BP; polysaccharides or proteins), humic substances fraction (HSF; humic and fulvic acid fraction), building blocks (BB; lower weight humic substances), low molecular weight neutrals (LMWN; aldehydes, small organic materials), and LMW-acids (LMWA; saturated mono-protic acids). A portion of the sample by-passes the SEC for determination of the overall DOC concentration, here referred to as DOM concentration in mg C/L. A number average molecular weight was derived only for the HSF based on elution time. Duplicates run at six concentrations yield a precision for the LC-OCD of <0.1 mg C/L for all fractions. Concentrations of each fraction were calculated using specialized software (ChromCALC, DOC-Labor, Germany) that integrated chromatograms from the LC-OCD.

Statistical analyses & Composition Wheel design

Samples from sites with multiple sampling events were averaged to create a single value per site. Data were analysed using unconstrained ordination analysis via principal components analysis (PCA) on a subset of samples that contained all composition measures listed in Table 1 (subset n=130). Data were scaled before PCA and analysed using R Statistical Software [42].

The Composition Wheel (CW) is a polygon drawn from axes of various composition measures that are independent of DOM concentration in order to focus solely on differences in DOM composition. Composition Wheel parameters were chosen based on the highest contribution of variables explaining the first two principal component axes (S1 Fig). Further, independent measures of DOM composition were preferentially chosen to minimize overlap in information between similar techniques. Each CW axis corresponds to a specific parameter. For each axis, the individual value for each sample is normalized as a value between the maximum and minimum encountered for that parameter within the dataset. All R code and data used to create the DOM CW, manuscript figures, and statistical analyses can be found at https://github.com/paukes/DOM-Comp-Wheel.

Results

DOM concentration & composition

DOM concentrations ranged from 0.1 to 273 mg C/L, with highest mean values in boreal groundwater, pond, and creek samples (Fig 2; S1 File). The highest DOM concentrations were found in groundwater environments in Yellowknife, while the lowest concentrations were found in high arctic environments (Fig 2). High arctic seeps, rivers, and lakes also generally had the lowest average DOC:DON values, but higher average specific ultra-violet absorbance at 255 nm (SUVA), spectral slope ($S_{275-295}$), and HSF values than other locations. SUVA and spectral slope values covered the known range as described broadly in the literature (SUVA: 1.1 to 21 L/(mg·m); spectral slope: 0.005 to 0.032 nm^{-1}). Highest SUVA values (>11 L/(mg·m)) were found at two sites: the anoxic bottom of a boreal lake and in the high arctic groundwater, but absorbance may be affected by high iron concentrations [14,43]. These two sites have unusually

high iron concentrations and were not included further in the discussion. Values of DOC:DON ranged between 9 to 124, and were lowest in rivers and high arctic samples. Humic substances fraction (HSF) ranged from 14% to 85% and on average were lowest in lakes. Overall, groundwater samples contained the highest DOC:DON and HSF values, and lowest $S_{275-295}$. Hence, both DOM concentration and composition varied across geographic scales and hydrological environments.

PCA on DOM composition measures

The first three principal component axes explained 66% of the variance in DOM composition using the measures contained in the dataset, with PC1 and PC2 accounting for 54% of the variability (Fig 3). Comparison of the first two principal components (PC) yield four distinct groupings of strongly-contributing measures: I) SUVA, SAC_{420}, SAC_{350}; II) HSF, HS MW; III) $S_{275-295}$, E_2:E_3, and S_R; and IV) BB, LMWN, and BP. Groups I and II were negatively associated to groups III and IV. Highest contributions to PC1 and PC2 axes were HSF, SAC_{350}, SAC_{420}, SUVA, and $S_{275-295}$. Variables with contribution to PC1 and PC2 lower than 2% were E_4:E_6, DOC:DON, $S_{350-400}$, and LMWA (Fig. S1). Absorbance parameters normalized to DOM concentrations (SAC_{350}, SAC_{420}, and SUVA) all plotted closely to each other and trended positively with measures of HSF, HSF molecular weight, and DOC:DON. Absorbance techniques plotted perpendicular to LC-OCD size fractions (Fig 3).

Based on contribution to the first two PC axes, we selected four DOM composition measures to define DOM composition. Further, these selected measures are quasi-independent as they are based on different analytical principles or attributes (SUVA, $S_{275-295}$: two different absorbance aspects; HSF: size-exclusion chromatography; DOC:DON: stoichiometry). Although the absorbance at different wavelengths within a sample are closely related [21], they

can be used to provide different information on DOM components as one characterizes the amount of UV-absorbing components normalized to DOM concentration at a specific wavelength (SUVA) while the other is associated with the shape of the absorbance spectra and varies with the distribution of DOM molecular weights ($S_{275-295}$). These four measures include three high-contributing variables to PC1 and PC2 axes (HSF, SUVA, and $S_{275-295}$). The length of the CW axis, and thus CW size, is dictated by the range of each compositional measure encountered in the entire dataset. Composition Wheels are then used as a basis for comparing DOM.

Shapes of Composition Wheels

Different environments are characterized by CW different shapes. Ponds and lakes tend to have lower values of SUVA and DOC:DON and higher $S_{275-295}$, resulting in a triangle shape elongated to the top-right corner (Fig 4). Groundwater DOM samples form a trapezoidal shape due to higher HSF and SUVA values than other sites. Differences in shape are found within locations between different hydrologic settings whereas similarities in shape are found within hydrological setting across locations. For instance, Yellowknife pond sites are similar in shape to groundwater DOM, while the creek, lake, and river shapes reflect DOM with higher $S_{275-295}$, lower DOC:DON, and lower HSF. Representation of different measures using these shapes allows for a facile comparison of DOM composition among samples.

Shapes also help to visualize and highlight the most extremes in DOM composition for each location. The spread of compositions is not evenly distributed between such extreme shapes at any given site but sampling was not targeted *a priori* based on shape. Most surface water sites contained a range in DOM composition between these extremes, forming either shapes similar to groundwater DOM or thin, elongated triangles in the $S_{275-295}$ direction. For this

reason, extremes were highlighted in sites with many different shapes to help identify a continuum of possible DOM sources or mixtures (Fig 4). Further, some sites did not conform to these end-members, as seen by the ELA creek sample with high DOC:DON, allowing easy identification of anomalous data or sites that may warrant further investigation.

Discussion

Comparison of DOM composition measures

Ranges in individual measures of DOM composition are large at both low and high concentrations of DOM (Fig 4, S2 Table) making it difficult to consistently separate sites or hydrological environments across different measures. For instance, accounting for both DOM concentration and DOC:DON may help differentiate some locations, but the range in DOC:DON values across moderate DOM concentrations covers most sites (Fig 2). Hence, new techniques that simultaneously consider different aspects of DOM composition, and are independent of concentration, are needed to compare variations in DOM composition across sample types and environments.

Different characterization techniques provide different information on DOM. In particular, the perpendicular relationship between absorbing and non-absorbing parameters observed among the first two PC axes indicate a range in different DOM properties are captured. For instance, all ELA creeks contain high and similar HSF values, yet we can use absorbance techniques based on molecular weight or UV-absorbing capability (via SUVA; Fig 2) to differentiate between these samples. However, correlations between size-based and absorbance parameters do not mean causation. For example, higher SUVA values are not consistently related to HSF proportions even though this is often assumed based on the higher aromaticity

and UV-absorbing capabilities of humic material [14,45]. Daring Lake creeks have high SUVA but low HSF. Although absorbance parameters are easily measured and helpful in comparing different DOM compositions, they do not accurately reflect non-absorbing components (e.g. stoichiometry or functional groups) that could differ among samples.

Effects of DOM Processes and CW End Members

Similar DOM CW shapes were found within hydrologic settings even though samples were collected from sites with varying climates and vegetation, spanning areas of boreal shield watersheds (IISD-ELA) to high arctic (Lake Hazen). Further, the range in values across the four CW measures compared well with DOM from other studies (i.e. similar DOM concentrations and SUVA values to rivers in the United States [16,44] and Canadian boreal lakes [46]) indicating that DOM composition and CW shape may not be unique to its locale. The similarity in CW shapes across different locations may result from analogous drivers of DOM fate. For instance, the proportion of biodegradable DOM was found to be a function of DOM composition and nutrients, rather than ecosystem or region-specific characteristics [47], suggesting that differences in the quality of DOM may not result from location alone. Hence, CWs can be used to amalgamate different compositional measures and quantify similarities in DOM sources and processing across a range of geomorphic, climate, and vegetation environments.

Composition Wheels can be further used to determine the degree of DOM degradation and facilitate comparisons of change along the aquatic continuum. This requires knowledge of the effect of processing, as well as the end-members (e.g. original sources of DOM). Microbial degradation of DOM induces a shift towards higher SUVA and lower DOC:DON (Fig 5; [48–51] but not $S_{275\text{-}295}$, resulting in a distinctive effect of microbial DOM transformation on the CW. Photolytic processing of DOM results in an increase in $S_{275\text{-}295}$ values and a general decrease in

the other three DOM quality measures [52–54]. Further, photolytic degradation affects all four compositional axes, whereas microbial degradation only affects two axes (Fig 5), indicating that certain measures of DOM composition respond differently to different DOM degradation processes. This has important implications for studies using single-characterization techniques as some parameters may not always faithfully serve as useful surrogates for others. For instance, microbial degradation changes SUVA but not HSF (Fig 5), even though SUVA has been linked to DOM aromaticity in humic substances [14]. Thus, comparative differences in a CW can help determine the dominant processes that produce the observed DOM composition of a sample. Further, knowing the degree DOM composition changes with photolysis allows CW to be used in a quantitative manner to quantify the amount of degradation. Although the quantitative response of DOM sources to photo- or microbial degradation is not yet sufficiently known across different environments, in areas where these rates of change to individual measures have been measured, CWs can be used in a quantitative manner to assess the extent and major processes contributing to DOM loss.

Laboratory experiments are useful to assess DOM source composition prior to extensive biotic or abiotic processing. Although this study did not conduct analysis on leachates, various studies have used similar DOM composition measures to identify DOM leachates. Leachates (organic matter steeped in de-ionized water) result in either low molecular weight, low aromatic DOM from mosses and coniferous sources [22,55] or large, humic, aromatic DOM components from other plant material and deciduous leaf litter [37,57,58]. DOM produced from aquatic (primary production) consists of low molecular weight, high protein and nitrogen content, and low UV-absorbing components and is thought to be rapidly consumed [37,56,59,60]. These parameters can also be represented by a CW (Figure 5b – using a range in values based on what

is presented in literature), and provide a shape to compare DOM origins from aquatic primary production versus terrestrial plants.

Two dominant DOM compositional end-member shapes are evident in our dataset: groundwater DOM sources and DOM altered by photolysis. Other shapes are intermediate between these two distinctive end-members. Degradation in groundwater in organic-rich substrates allows for the accumulation of large, aromatic components of DOM (high HSF, SUVA, and low $S_{275-295}$; [61]), resulting in a large trapezoid shape CW. This trapezoid shape is consistent for groundwater DOM across most sites, supporting previous groundwater studies that attribute the narrow DOM compositional range to groundwater processing [23]. In contrast, a 'kite-like' shape results from the effects of photolysis (Fig 4), resulting in DOM with lower molecular weight and less UV-absorbing components [15]. Further, photolysis end-member CWs are similar in shape to the end-products of photolytic experiments (Fig 5; [51]), and are clearly seen in surface waters across all sites (Fig 4). Hence, these end-member shapes may constrain the possible range in CW shapes that can be found within aquatic environments.

The groundwater/photolysis end-member categorization frames our conceptual model (Fig 6) that quantifies how the two end-member CW shapes evolve depending on the aquatic-terrestrial hydrologic connection (Fig 6; pathway A-b) or exposure to sunlight (Fig 6: pathway A-B). For instance, creeks with little to no processing of groundwater-derived DOM can be identified by CW shapes similar to groundwater DOM, as seen in ELA and some Daring creeks (Fig 4). ELA lakes have a wide gradient of CW shape and thus overall DOM quality (Fig 4). The use of CW to pair process-based knowledge of DOM composition with hydrologic transport provides a framework that can be used identify key knowledge gaps (i.e. rates of degradation, kinetics based

on composition, relative organic source contributions, water residence time) and quantify the relationship between DOM sources and degree of processing within the environment.

Certain creeks and rivers from YK or WK do not fit into the end-member categories as they contain shapes with larger right sides (higher $S_{275\text{-}295}$ and SUVA than other samples), indicating other processes may be important in determining DOM composition. This may be a result of our sampling of mostly oligotrophic systems that are dominated by terrestrial carbon. We hypothesize that these different shapes represent surface water systems with greater *in-situ*, or autochthonous, contributions of DOM, generally characterized by higher amounts of proteins and smaller molecular weight components [62–64]. Thus, although our dataset was not comprehensive in terms of capturing the full range of DOM sources, the CW-informed conceptual model provides an initial framework to build the factors leading to a specific DOM composition.

Adaptability of DOM Composition Wheels

Expressing DOM composition with only four concentration-independent parameters excludes advantages of other techniques not used in this study. However, agreement between multiple parameters allows for selection of surrogates for the CW. LC-OCD is not as widely available but many studies have traditionally used resins [16,65,66] or other size-exclusion columns [67,68] to characterize DOM. Further, LC-OCD fractions of humics have been well correlated to measures of ^{13}C-NMR and fluorescence measures such as HIX [12,69,70]. Although fluorescence was not used in this study, strong associations between certain fluorescence parameters and absorbance or molecular-weight groupings could be used to replace LC-OCD defined fractions, such as using PARAFAC modelling to discern components most similar to HSF [12,70] (Fig 7). These fluorescence parameters are also independent measures of

DOM composition and could be readily substituted into the CW. Elemental ratios of DOC:DON are generally positively correlated with humic-like fluorescence and negatively correlated to protein-like components [71]. Other absorbance indices such as slope ratio and E_2:E_3 (Table 1) are potential surrogates for $S_{275\text{-}295}$ (Fig 2), providing various parameters that can be substituted for one another when comparing studies where only one of these measures is provided. Measurements of SUVA could be substituted with SAC_{420}, SAC_{350}, or E_4:E_6 [25,71]. However, although SUVA has been correlated with HIX and to fluorescence component C3 [25,71], the opposite has also been found [70]. Composition Wheels can easily incorporate advanced techniques, such as FT-ICR-MS, that can provide information on the molecular heterogeneity of DOM, identification of either terrestrial-like (via condensed and polycyclic aromatics or polyphenolic compounds) or *in situ* DOM sources (higher aliphatic and peptide-like compounds), or to identify differences in H:C and O:C due to microbial or photodegradation [12,13,72]. Associations between different characterization techniques allow for mixing of techniques and comparison of different variables, indicating a wide-range of applicability of CW within environmental sciences.

The CW visualization method provides an efficient communication tool not only among scientists, but also between scientists and other stakeholders concerned with water quality, including community members. Shapes from CWs show clearly how DOM differs, whereas changes in the numerical value of multiple metrics are only easily grasped by those with familiarity with the methods and environmental ranges. Further work could include pairing different shapes of DOM with key DOM roles such as disinfection demand and by-product formation, metal mobility, and mercury bioaccumulation. By reducing the complexity of

independent DOM measures and creating an easily comparable shape, differences in DOM composition can be easily grasped and communicated to larger audiences.

Acknowledgements

We thank Michael English, Roy Judas, and Jordan Reid for field assistance in collecting samples in the Northwest Territories; Paul Dainard, Kyra St. Pierre, Igor Lehnherr, Vince St. Louis, Jessica Serbu, Maria Cavacao, Victoria Wisniewski, and Michael English for field assistance at Lake Hazen, NU; Will Robertson for assistance at Long Point, ON; Environmental Geochemistry Lab, University of Waterloo for sampling the Grand River, ON; John Spoelstra for sampling Black Brook Watershed, Nottawasaga River Watershed, and Turkey Lakes Watershed. We also thank the Community of Wekweètì and the Wek'èezhìi Land & Water Board for their support, and the Community-Based Monitoring Program and Department of Environment and Natural Resources, Government of Northwest Territories, for collection of samples from the Mackenzie River, NT. We would like thank Richard J. Elgood for logistical, field, and technical help, Monica Tudorancea assistance with the LC-OCD analysis, and Mackenzie Schultz for help with Figure 1. We are grateful for the high arctic logistic support provided by Parks Canada, and funding from the Polar Continental Shelf Program (PCSP), Northwest Territories Cumulative Impact Monitoring Program, Northern Scientific Training Program, and the National Science and Engineering Research Council of Canada. We thank Igor Lehnherr, Susan Ziegler, Chris Parsons, Roland Hall, and three anonymous reviewers for their comments on earlier drafts of this manuscript. PJKA also benefitted from scholarships from the Garfield Weston Foundation, TD Friends of the Environment, and the University of Waterloo. Data used in this manuscript can be found in the publicly-available Wilfrid Laurier University Scholars Portal Dataverse (https://doi.org/10.5683/SP2/NG6D02), while all R code used for statistical analyses, figure

creation, and a Composition Wheel template is available from https://github.com/paukes/DOM-Comp-Wheel.

References

1. Strock KE, Theodore N, Gawley WG, Ellsworth AC, Saros JE. Increasing dissolved organic carbon concentrations in northern boreal lakes: Implications for lake water transparency and thermal structure. J Geophys Res Biogeosciences. 2017;122: 1022–1035. doi:10.1002/2017JG003767
2. Baken S, Degryse F, Verheyen L, Merckx R, Smolders E. Metal complexation properties of freshwater dissolved organic matter are explained by its aromaticity and by anthropogenic ligands. Environ Sci Technol. 2011;45: 2584–2590. doi:10.1021/es103532a
3. Bauer M, Heitmann T, Macalady DL, Blodau C. Electron transfer capacities and reaction kinetics of peat dissolved organic matter. Environ Sci Technol. 2007;41: 139–145. doi:10.1021/es061323j
4. Matilainen A, Gjessing ET, Lahtinen T, Hed L, Bhatnagar A, Sillanpää M. An overview of the methods used in the characterisation of natural organic matter (NOM) in relation to drinking water treatment. Chemosphere. 2011;83: 1431–1442. doi:10.1016/j.chemosphere.2011.01.018
5. Krasner SW, Weinberg HS, Richardson SD, Pastor SJ, Chinn R, Sclimenti MJ, et al. Occurrence of a New Generation of Disinfection Byproducts. Environ Sci Technol. 2006;40: 7175–7185. doi:10.1021/es060353j
6. Evans CD, Monteith DT, Cooper DM. Long-term increases in surface water dissolved organic carbon: observations, possible causes and environmental impacts. Environ Pollut. 2005;137: 55–71. doi:10.1016/j.envpol.2004.12.031
7. Weyhenmeyer GA, Prairie YT, Tranvik LJ. Browning of boreal freshwaters coupled to carbon-iron interactions along the aquatic continuum. PLoS One. 2014;9: e88104. doi:10.1371/journal.pone.0088104
8. Worrall F, Burt TP. Changes in DOC treatability: Indications of compositional changes in DOC trends. J Hydrol. 2009;366: 1–8. doi:10.1016/j.jhydrol.2008.11.044
9. Ritson JP, Graham NJD, Templeton MR, Clark JM, Gough R, Freeman C. The impact of climate change on the treatability of dissolved organic matter (DOM) in upland water supplies: A UK perspective. Sci Total Environ. 2014;473–474: 714–730. doi:10.1016/j.scitotenv.2013.12.095
10. Creed IF, Bergström AK, Trick CG, Grimm NB, Hessen DO, Karlsson J, et al. Global change-driven effects on dissolved organic matter composition: Implications for food webs of northern lakes. Glob Chang Biol. 2018;24: 3692–3714. doi:10.1111/gcb.14129
11. Larsen LG, Aiken GR, Harvey JW, Noe GB, Crimaldi JP. Using fluorescence spectroscopy to trace seasonal DOM dynamics, disturbance effects, and hydrologic transport in the Florida Everglades. J Geophys Res. 2010;115: 1–14. doi:10.1029/2009JG001140
12. Hutchins RHS, Aukes PJK, Schiff SL, Dittmar T, Prairie YT, del Giorgio PA. The Optical, Chemical, and Molecular Dissolved Organic Matter Succession Along a Boreal Soil-Stream-River Continuum. J Geophys Res Biogeosciences. 2017;122: 2892–2908.

doi:10.1002/2017JG004094

13. Kellerman AM, Guillemette F, Podgorski DC, Aiken GR, Butler KD, Spencer RGM. Unifying Concepts Linking Dissolved Organic Matter Composition to Persistence in Aquatic Ecosystems. Environ Sci Technol. 2018;52: 2538–2548. doi:10.1021/acs.est.7b05513
14. Weishaar JL, Aiken GR, Bergamaschi BA, Fram MS, Fujii R, Mopper K. Evaluation of specific ultraviolet absorbance as an indicator of the chemical composition and reactivity of dissolved organic carbon. Environ Sci Technol. 2003;37: 4702–4708. doi:10.1021/es030360x
15. Helms JR, Stubbins A, Ritchie JD, Minor EC, Kieber DJ, Mopper K. Absorption spectral slopes and slope ratios as indicators of molecular weight, source, and photobleaching of chromophoric dissolved organic matter. Limnol Oceanogr. 2008;53: 955–969. doi:10.4319/lo.2008.53.3.0955
16. Spencer RGM, Butler KD, Aiken GR. Dissolved organic carbon and chromophoric dissolved organic matter properties of rivers in the USA. J Geophys Res Biogeosciences. 2012;117. doi:10.1029/2011JG001928
17. Stedmon C a, Markager S, Bro R. Tracing dissolved organic matter in aquatic environments using a new approach to fluorescence spectroscopy. Mar Chem. 2003;82: 239–254. doi:10.1016/S0304-4203(03)00072-0
18. Jaffé R, Yamashita Y, Maie N, Cooper WT, Dittmar T, Dodds WK, et al. Dissolved Organic Matter in Headwater Streams: Compositional Variability across Climatic Regions of North America. Geochim Cosmochim Acta. 2012;94: 95–108. doi:10.1016/j.gca.2012.06.031
19. Hunt AP, Parry JD, Hamilton-Taylor J. Further evidence of elemental composition as an indicator of the bioavailability of humic substances to bacteria. Limnol Oceanogr. 2000;45: 237–241.
20. Huber SA, Balz A, Abert M, Pronk W. Characterisation of aquatic humic and non-humic matter with size-exclusion chromatography – organic carbon detection – organic nitrogen detection (LC-OCD-OND). Water Res. 2011;45: 879–885. doi:10.1016/j.watres.2010.09.023
21. Massicotte P, Asmala E, Stedmon C, Markager S. Global distribution of dissolved organic matter along the aquatic continuum: Across rivers, lakes and oceans. Sci Total Environ. 2017;609: 180–191. doi:10.1016/j.scitotenv.2017.07.076
22. Wickland KP, Neff JC, Aiken GR. Dissolved Organic Carbon in Alaskan Boreal Forest: Sources, Chemical Characteristics, and Biodegradability. Ecosystems. 2007;10: 1323–1340. doi:10.1007/s10021-007-9101-4
23. Shen Y, Chapelle FH, Strom EW, Benner R. Origins and bioavailability of dissolved organic matter in groundwater. Biogeochemistry. 2015;122: 61–78. doi:10.1007/s10533-014-0029-4
24. Aukes PJK, Schiff SL, Robertson WD. Evolution of Dissolved Organic Matter Along a Septic System Plume: Evidence of Sustained Biogeochemical Activity in the Groundwater Zone. J Geophys Res Biogeosciences. 2019;124: 1389–1400. doi:10.1029/2018JG004758
25. Kellerman AM, Kothawala DN, Dittmar T, Tranvik LJ. Persistence of dissolved organic matter in lakes related to its molecular characteristics. Nat Geosci. 2015;8. doi:10.1038/ngeo2440
26. Kellerman AM, Dittmar T, Kothawala DN, Tranvik LJ. Chemodiversity of dissolved

organic matter in lakes driven by climate and hydrology. Nat Commun. 2014;5: 1–8. doi:10.1038/ncomms4804

27. Creed IF, Mcknight DM, Pellerin BA, Green MB, Bergamaschi BA, Aiken GR, et al. The river as a chemostat : fresh perspectives on dissolved organic matter flowing down the river continuum. Can J Fish Aquat Sci. 2015;14: 1–14.
28. McCallister SL, Ishikawa NF, Kothawala DN. Biogeochemical tools for characterizing organic carbon in inland aquatic ecosystems. Limnol Oceanogr Lett. 2018;3: 444–457. doi:10.1002/lol2.10097
29. Pinker S. Theory of Graph Comprehension. In: Freedle R, editor. Artificial intelligence and the future of testing. Lawrence Erlbaum Associates, Inc.; 1990. pp. 73–126.
30. Zhu B, Watts SA. Visualization of network concepts: The impact of working memory capacity differences. Inf Syst Res. 2010;21: 327–344. doi:10.1287/isre.1080.0215
31. Gordin DN, Pea RD. Prospects for Scientific Visualization as an Educational Technology. J Learn Sci. 1995;4: 249–279.
32. Pauwels L. An integrated model for conceptualising visual competence in scientific research and communication. Vis Stud. 2008;23: 147–161. doi:10.1080/14725860802276305
33. Martin LJ, Turnquist A, Groot B, Huang SYM, Kok E, Thoma B, et al. Exploring the Role of Infographics for Summarizing Medical Literature. Heal Prof Educ. 2019;5: 48–57. doi:10.1016/j.hpe.2018.03.005
34. Shamoun-Baranes J, Farnsworth A, Aelterman B, Alves JA, Azijn K, Bernstein G, et al. Innovative visualizations shed light on avian nocturnal migration. PLoS One. 2016;11: 1–15. doi:10.1371/journal.pone.0160106
35. Lupi G, Accurat. Beautiful Reasons - Engaging Aesthetics for Data Narratives [Internet]. 2016 [cited 18 Jan 2020]. Available: https://medium.com/accurat-studio/beautiful-reasons-c1c6926ab7d7
36. Lundin EJ, Klaminder J, Bastviken D, Olid C, Hansson S V., Karlsson J. Large difference in carbon emission - Burial balances between boreal and arctic lakes. Sci Rep. 2015;5: 1–7. doi:10.1038/srep14248
37. Hansen AM, Kraus TEC, Pellerin BA, Fleck JA, Downing BD, Bergamaschi BA. Optical properties of dissolved organic matter (DOM): Effects of biological and photolytic degradation. Limnol Oceanogr. 2016;61: 1015–1032. doi:10.1002/lno.10270
38. Marshall IB, Schut PH, Ballard M. A National Ecological Framework for Canada: Attribute Data [Internet]. Ottawa, ON, Canada: Ecosystem Stratification Working Group, Agriculture and Agri-Food Canada & Environment Canada; 1999. Available: http://sis.agr.gc.ca/cansis/nsdb/ecostrat/1999report/index.html
39. Dahlén J, Bertilsson S, Pettersson C. Effects of UV-A radiation on dissolved organic matter in humic surface waters. Environ Int. 1996;22: 501–506.
40. Chin Y-P, Aiken GR, O'Loughlin E. Molecular Weight, Polydispersity, and Spectroscopic Properties of Aquatic Humic Substances. Environ Sci Technol. 1994;28: 1853–1858. doi:10.1021/es00060a015
41. Curtis PJ, Schindler DW. Hydrologic control of dissolved organic matter in low-order Precambrian Shield lakes. Biogeochemistry. 1997;36: 125–138. doi:10.1023/A:1005787913638
42. R Core Team. R: A language and environment for statistical computing. [Internet]. Vienna, Austria: R Foundation for Statistical Computing; 2020. Available: http://www.r-

project.org
43. Poulin B a, Ryan JN, Aiken GR. Effects of Iron on Optical Properties of Dissolved Organic Matter. Environ Sci Technol. 2014; 1–20. doi:10.1021/es502670r
44. Jaffé R, McKnight D, Maie N, Cory RM, McDowell WH, Campbell JL. Spatial and temporal variations in DOM composition in ecosystems: The importance of long-term monitoring of optical properties. J Geophys Res. 2008;113: 1–15. doi:10.1029/2008JG000683
45. Hua G, Reckhow DA, Abusallout I. Correlation between SUVA and DBP formation during chlorination and chloramination of NOM fractions from different sources. Chemosphere. 2015;130: 82–89. doi:10.1016/j.chemosphere.2015.03.039
46. Mueller KK, Fortin C, Campbell PGC. Spatial Variation in the Optical Properties of Dissolved Organic Matter (DOM) in Lakes on the Canadian Precambrian Shield and Links to Watershed Characteristics. Aquat Geochemistry. 2012;18: 21–44. doi:10.1007/s10498-011-9147-y
47. Lapierre J-F, del Giorgio PA. Partial coupling and differential regulation of biologically and photochemically labile dissolved organic carbon across boreal aquatic networks. Biogeosciences. 2014;11: 5969–5985. doi:10.5194/bg-11-5969-2014
48. Koehler B, Von Wachenfeldt E, Kothawala DN, Tranvik LJ. Reactivity continuum of dissolved organic carbon decomposition in lake water. J Geophys Res Biogeosciences. 2012;117: 1–14. doi:10.1029/2011JG001793
49. McDowell WH, Zsolnay A, Aitkenhead-Peterson J, Gregorich EG, Jones DL, Jödemann D, et al. A comparison of methods to determine the biodegradable dissolved organic carbon from different terrestrial sources. Soil Biol Biochem. 2006;38: 1933–1942. doi:10.1016/j.soilbio.2005.12.018
50. Kalbitz K, Schwesig D, Schmerwitz J, Kaiser K, Haumaier L, Glaser B, et al. Changes in properties of soil-derived dissolved organic matter induced by biodegradation. Soil Biol Biochem. 2003;35: 1129–1142. doi:10.1016/S0038-0717(03)00165-2
51. Aukes PJK. Dissolved Organic Matter in the Canadian Arctic & Sub-Arctic: Importance of DOM Quality & Quantity in a Warming Climate. University of Waterloo. 2019.
52. Winter AR, Fish TAE, Playle RC, Smith DS, Curtis PJ. Photodegradation of natural organic matter from diverse freshwater sources. Aquat Toxicol. 2007;84: 215–222. doi:10.1016/j.aquatox.2007.04.014
53. Franke D, Hamilton MW, Ziegler SE. Variation in the photochemical lability of dissolved organic matter in a large boreal watershed. Aquat Sci. 2012;74: 751–768. doi:10.1007/s00027-012-0258-3
54. Mann PJ, Davydova a., Zimov NS, Spencer RGM, Davydov S, Bulygina E, et al. Controls on the composition and lability of dissolved organic matter in Siberia's Kolyma River basin. J Geophys Res. 2012;117: G01028. doi:10.1029/2011JG001798
55. Sun L, Perdue EM, Meyer JL, Weis J. Use of elemental composition to predict bioavailability dissolved organic matter in a Georgia river. Limnol Oceanogr. 1997;42: 714–721. doi:10.4319/lo.1997.42.4.0714
56. Catalán N, Obrador B, Felip M, Pretus JL. Higher reactivity of allochthonous vs. autochthonous DOC sources in a shallow lake. Aquat Sci. 2013;75: 581–593. doi:10.1007/s00027-013-0302-y
57. Lee M-H, Hur J. Photodegradation-Induced Changes in the Characteristics of Dissolved Organic Matter with Different Sources and Their Effects on Disinfection By-Product

Formation Potential. CLEAN - Soil, Air, Water. 2014;42: 552–560. doi:10.1002/clen.201200685

58. Singh S, Inamdar S, Mitchell MJ, McHale P. Seasonal pattern of dissolved organic matter (DOM) in watershed sources : influence of hydrologic flow paths and autumn leaf fall. Biogeochemistry. 2014;118: 321–337. doi:10.1007/s10533-013-9934-1

59. Pivokonsky M, Safarikova J, Baresova M, Pivokonska L, Kopecka I. A comparison of the character of algal extracellular versus cellular organic matter produced by cyanobacterium, diatom and green alga. Water Res. 2014;51: 37–46. doi:10.1016/j.watres.2013.12.022

60. McKnight DM, Andrews ED, Spaulding SA, Aiken GR. Aquatic fulvic acids in algal-rich antarctic ponds. Limnol Oceanogr. 1994;39: 1972–1979. doi:10.4319/lo.1994.39.8.1972

61. Wauthy M, Rautio M, Christoffersen KS, Forsström L, Laurion I, Mariash HL, et al. Increasing dominance of terrigenous organic matter in circumpolar freshwaters due to permafrost thaw. Limnol Oceanogr Lett. 2018; doi:10.1002/lol2.10063

62. Tank SE, Lesack LFW, Gareis J a. L, Osburn CL, Hesslein RH. Multiple tracers demonstrate distinct sources of dissolved organic matter to lakes of the Mackenzie Delta, western Canadian Arctic. Limnol Oceanogr. 2011;56: 1297–1309. doi:10.4319/lo.2011.56.4.1297

63. Roiha T, Peura S, Cusson M, Rautio M. Allochthonous carbon is a major regulator to bacterial growth and community composition in subarctic freshwaters. Sci Rep. 2016;6: 34456. doi:10.1038/srep34456

64. Hood E, Fellman JB, Spencer RGM, Hernes PJ, Edwards R, D'Amore D V., et al. Glaciers as a source of ancient and labile organic matter to the marine environment. Nature. 2009;462: 1044–7. doi:10.1038/nature08580

65. Cleveland CC, Neff JC, Townsend AR, Hood E. Composition, Dynamics, and Fate of Leached Dissolved Organic Matter in Terrestrial Ecosystems: Results from a Decomposition Experiment. Ecosystems. 2004;7: 275–285. doi:10.1007/s10021-003-0236-7

66. Bourbonniere R. Distribution patterns of dissolved organic matter fractions in natural waters from eastern Canada. Org Geochem. 1989;14: 97–107. doi:10.1016/0146-6380(89)90023-5

67. Her N, Amy GL, Foss D, Cho J, Yoon Y, Kosenka P. Optimization of method for detecting and characterizing NOM by HPLC-size exclusion chromatography with UV and on-line DOC detection. Environ Sci Technol. 2002;36: 1069–76. Available: http://www.ncbi.nlm.nih.gov/pubmed/11917993

68. Kawasaki N, Matsushige K, Komatsu K, Kohzu A, Nara FW, Ogishi F, et al. Fast and precise method for HPLC-size exclusion chromatography with UV and TOC (NDIR) detection: importance of multiple detectors to evaluate the characteristics of dissolved organic matter. Water Res. 2011;45: 6240–6248. doi:10.1016/j.watres.2011.09.021

69. Romera-Castillo C, Chen M, Yamashita Y, Jaffé R. Fluorescence characteristics of size-fractionated dissolved organic matter: Implications for a molecular assembly based structure? Water Res. 2014;55C: 40–51. doi:10.1016/j.watres.2014.02.017

70. Bodmer P, Heinz M, Pusch M, Singer GA, Premke K. Carbon dynamics and their link to dissolved organic matter quality across contrasting stream ecosystems. Sci Total Environ. 2016;553: 574–586. doi:10.1016/j.scitotenv.2016.02.095

71. Kothawala DN, Stedmon CA, Müller RA, Weyhenmeyer GA, Köhler SJ, Tranvik LJ.

Controls of dissolved organic matter quality: Evidence from a large-scale boreal lake survey. Glob Chang Biol. 2014;20: 1101–1114. doi:10.1111/gcb.12488

72. Ward CP, Nalven SG, Crump BC, Kling GW, Cory RM. Photochemical alteration of organic carbon draining permafrost soils shifts microbial metabolic pathways and stimulates respiration. Nat Commun. 2017; 1–8. doi:10.1038/s41467-017-00759-2

Tables

Table 1. Dissolved organic matter composition as described by chemical, absorbance, and molecular-size based measures used in this study.

Measure (*common abbreviation*)	Equation	Unit	Characteristic	Reference
Chemical				
DOC:DON	$M_C \div M_N$	-	Stoichiometry	[19]
Absorbance				
E_2:E_3	$A_{255} \div A_{365}$	-	Inversely related to molecular size	[39]
E_4:E_6	$A_{465} \div A_{665}$	-	Humic molecular weight and size	[40]
SAC_{350}	$\frac{ln(10) \times A_{420}/L}{[DOC]}$	$\frac{cm^2}{mg\text{-}C} \div 10^3$	Specific absorbance at 350 nm and attributed to colour	[41]
SAC_{420}	$\frac{ln(10) \times A_{420}/L}{[DOC]}$	$\frac{L}{mg \times m}$	Specific absorbance at 420 nm	
SUVA	$\frac{ln(10) \times A_{255}/L}{[DOC]}$	$\frac{L}{mg \times m}$	Correlated to degree of aromaticity	[14]
$S_{275\text{-}295}$	$a_\lambda = a_{\lambda_{275}} e^{-S(\lambda-275)}$	nm^{-1}	Inversely related to MW (where *S* is the slope)	[15]
$S_{350\text{-}400}$	$a_\lambda = a_{\lambda_{350}} e^{-S(\lambda-350)}$	nm^{-1}	Used with $S_{275\text{-}295}$ to calculated S_R	[15]
S_R	$\frac{S_{275-295}}{S_{350-400}}$	-	Inversely related to overall molecular weight; integrative indicator of light-absorbing DOM history	[15]
Size Exclusion Chromatography				
Biopolymers (BP)	-	% of DOM	Polysaccharides, proteins	[20]
Humic substances (HSF)	-	% of DOM	Humic or fulvic-like components	[20]
Building Blocks (BB)	-	% of DOM	Degraded HS	[20]
Low-molecular weight neutrals (LMWN)	-	% of DOM	Aldehydes, small organic materials	[20]
Low-molecular weight acids (LMWA)	-	% of DOM	Saturated mono-protic acids	[20]
HS molecular weight (HS MW)	-	g / mol	Nominal average molecular weight of HS	[20]

Figure

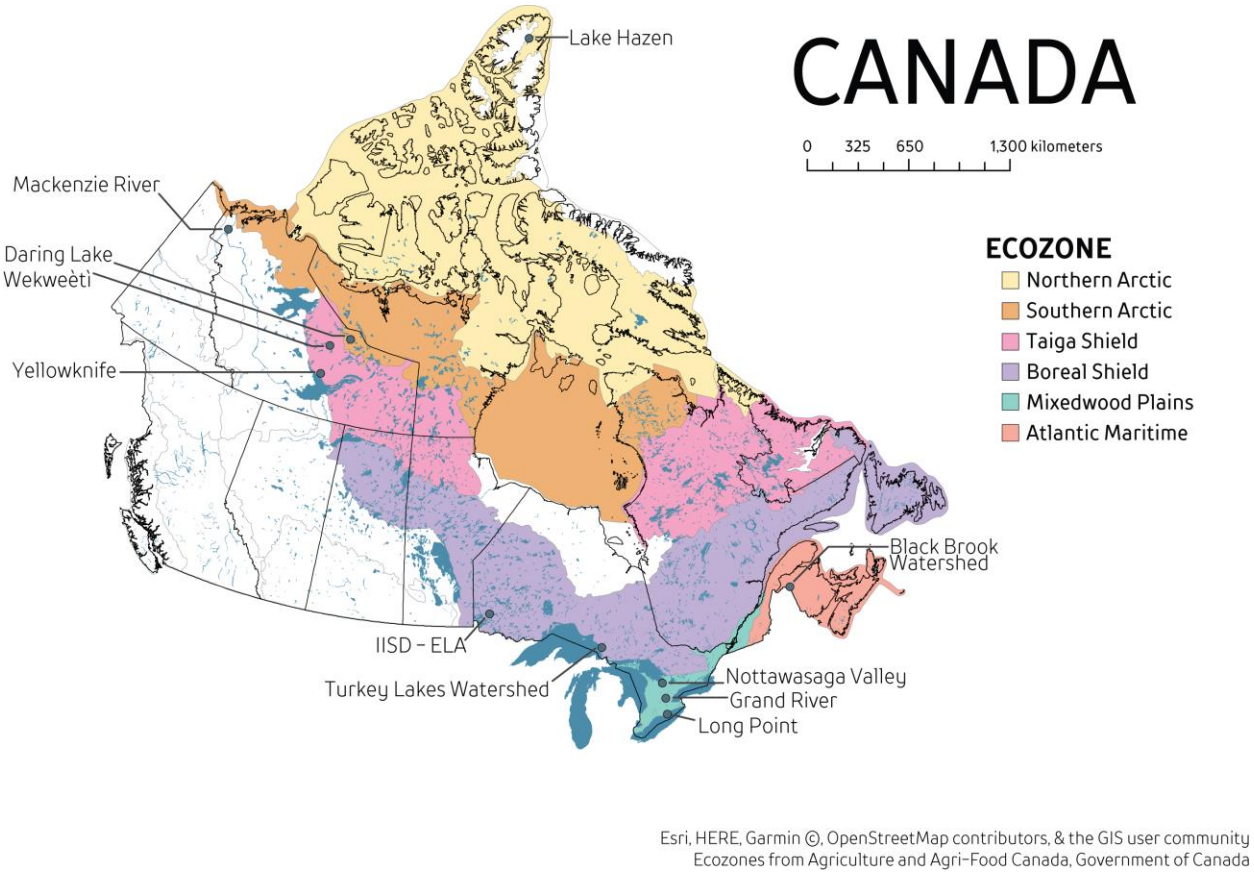

Fig 1. Locations of sampling sites and ecozones. River locations (Grand River, ON; Mackenzie River, NT) are labelled at the mouth of the river.

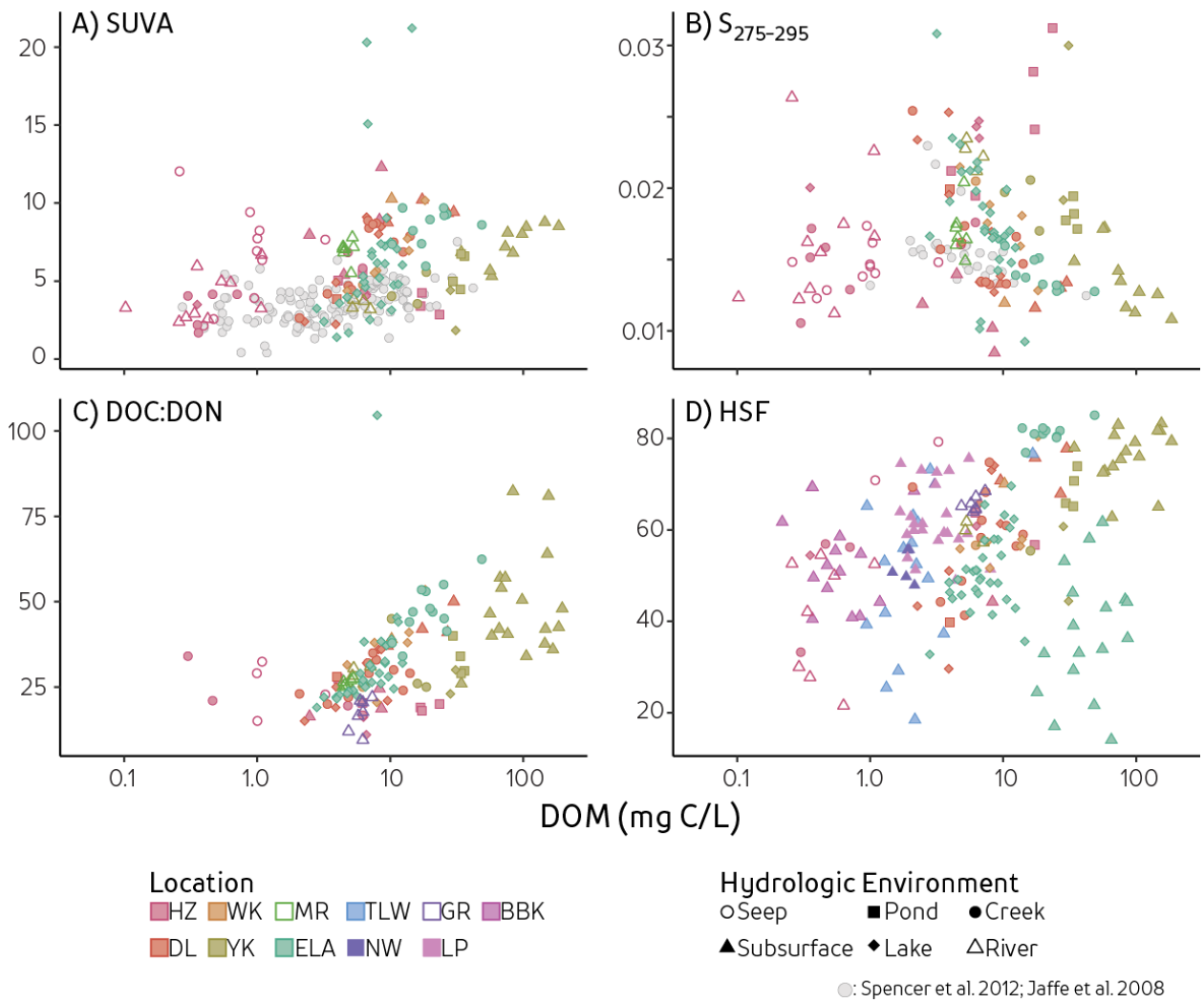

Fig 2. Compositional measures versus total DOM concentration. Measures include A) SUVA, specific ultraviolet absorbance at 255 nm, B) $S_{275\text{-}295}$, spectral slope between 275 to 295nm, C) DOC:DON, and D) HSF; humic substances fraction. Colours represent geographical sampling locations (HZ: Lake Hazen Watershed, NU; DL: Daring Lake, NT; WK: Wekweètì, NT; YK: Yellowknife, NT; MR: Mackenzie River, NT; ELA: IISD-Experimental Lakes Area, ON; TLW: Turkey Lakes Watershed, ON; NW: Nottawasaga River Watershed, ON; GR: Grand River, ON; LP: Long Point, ON; BBK: Black Brook Watershed, ON) while shapes represent hydrologic environments. Light grey circles represent two other published DOM characterization studies conducted at similar scales [16,44].

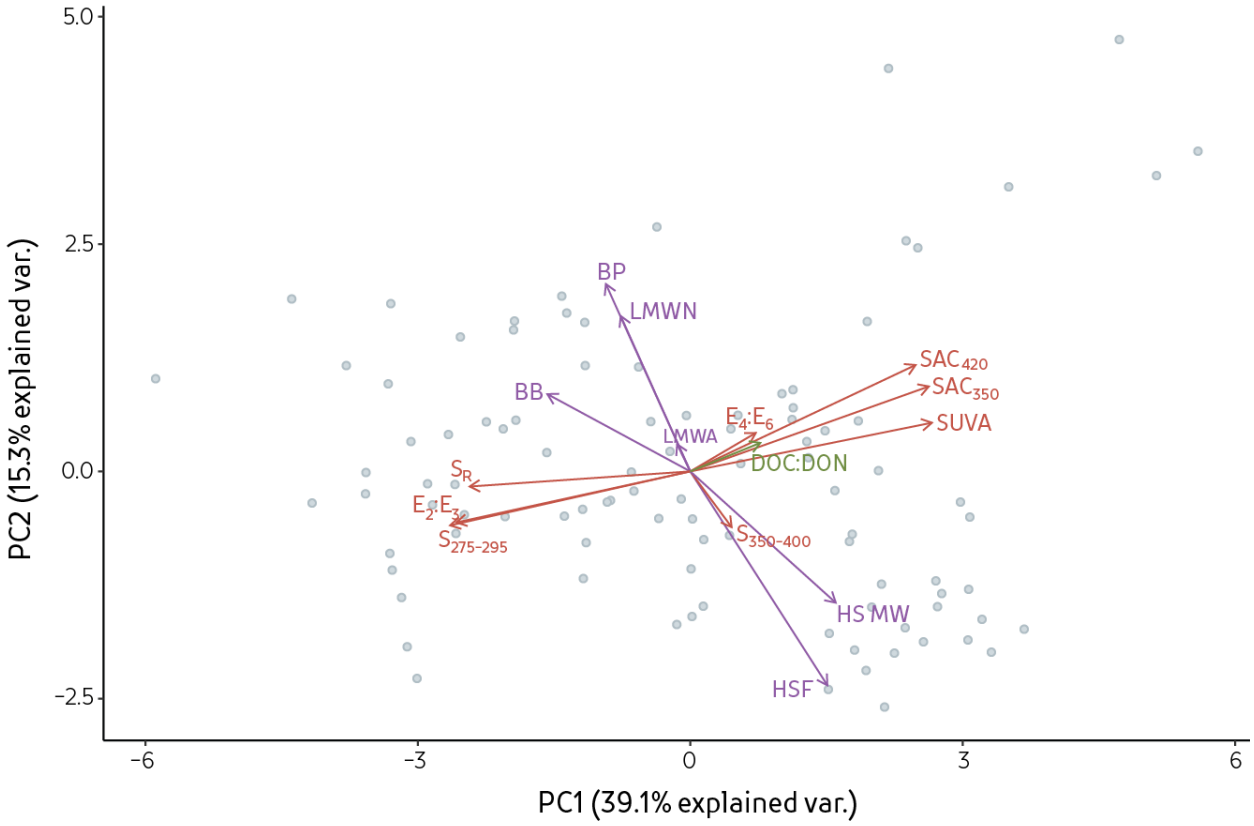

Fig 3. Principal component analyses for samples from different ecozones. Grey dots represent individual samples, while vectors represent absorbance (red), elemental (green), and LC-OCD (purple) compositional measures.

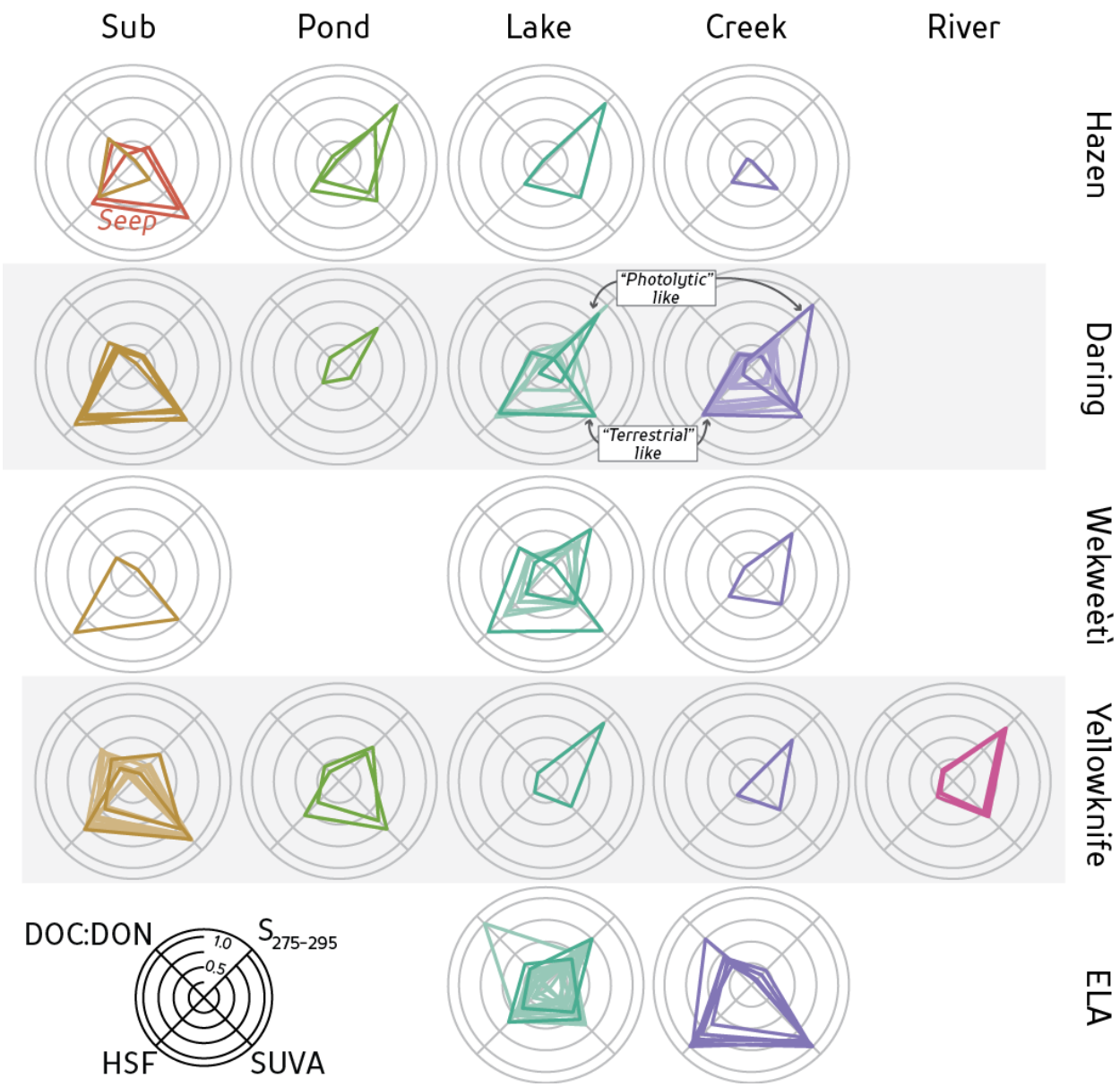

Fig 4. Composition wheels for DOM from different hydrologic settings within each geographical site. Axes are a numerical value normalized relative to the maximum and minimum encountered within the dataset for each parameter. Parameters for each axis found in bottom left. The orientation of the composition wheel (CW) axes are arbitrary. Different samples from the same hydrological and geographic setting are plotted within the same CW. Two 'end member' compositions are highlighted in sites with many samples to help visualize the continuum of DOM mixtures: groundwater-like DOM (low DOC:DON, high SUVA and HSF) or photolyzed DOM (high $S_{275-295}$).

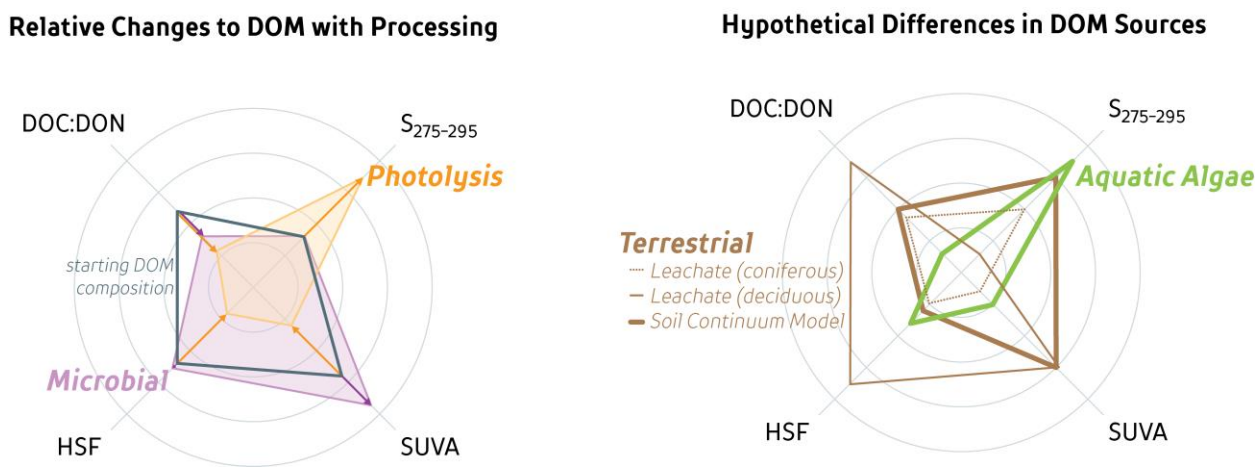

Fig 5. Changes to a Composition Wheel resulting from photolytic and microbial degradation (left) and differences in terrestrial versus aquatic DOM sources (right). Changes to dissolved organic matter (DOM) (grey) with photolytic (orange; 12 to 18 day exposure to sunlight) or microbial (purple; 30-day experiment) degradation based on experimental incubations of natural DOM samples [51] (left). The mean decrease in DOC concentration was 18% during photolysis and 10% during microbial degradation experiments (n=11, 9; respectively). Hypothetical differences in DOM sources (right) are based on various leachate experiments in literature [22,37,55–59].

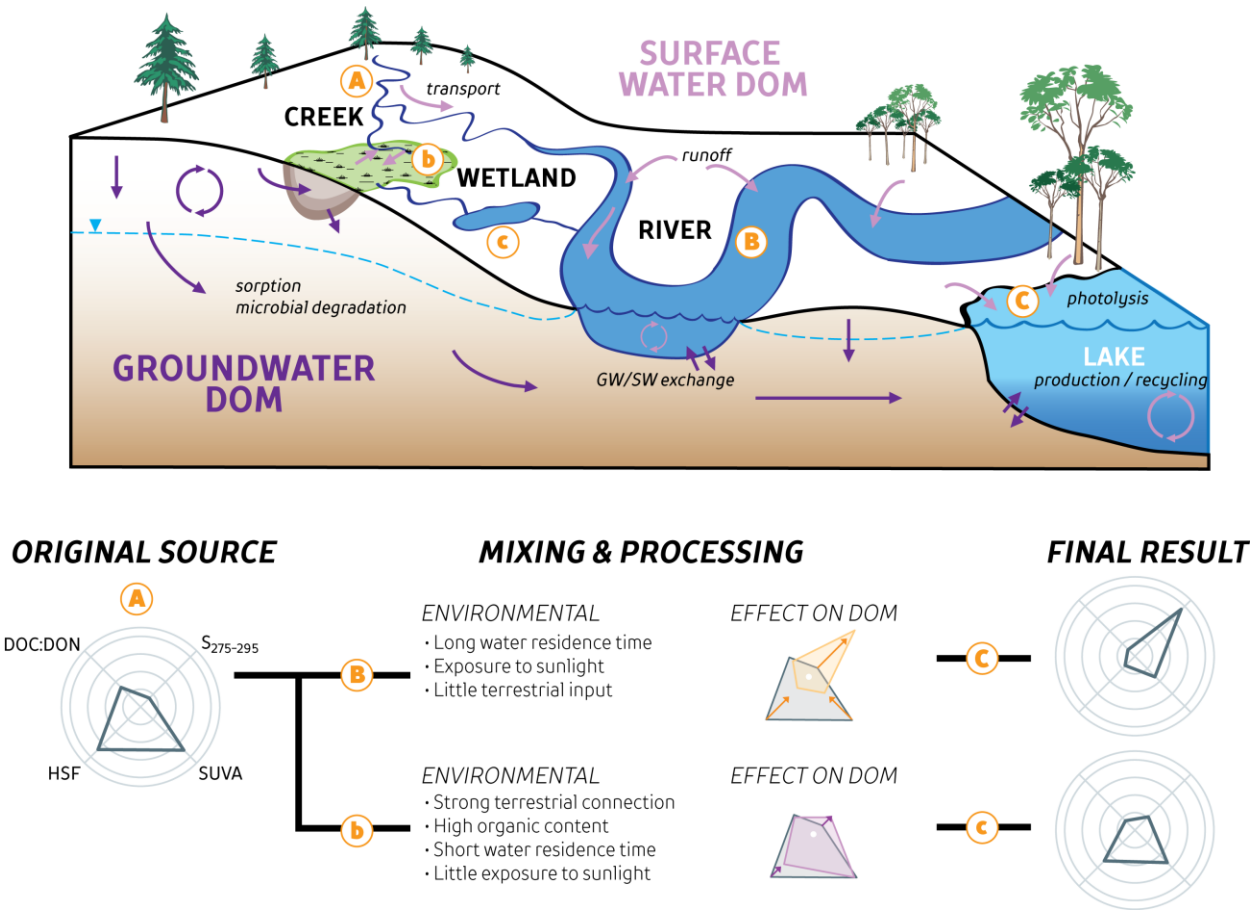

Fig 6. Conceptual model of DOM evolution along the aquatic continuum using Composition Wheels. A conceptual model of a few select processes and sources of dissolved organic matter (DOM) along the aquatic continuum. Two main hydrologic flowpaths are illustrated (A-B-C and A-b-c) and originate from the same source 'A'. However, each flowpath undergoes different processing within the environment. Arrows represent the transport or addition of DOM among groundwaters (dark purple) and surface waters (light purple), while lowercase text highlights some of the specific processes and sources encountered. The wetland 'b' represents an area of organic matter degradation and DOM accumulation within organic-rich groundwaters, resulting in the transport of large, aromatic DOM components into surface water 'c'. Conversely, DOM is rapidly transported down the river 'B' and into a large lake 'C', resulting in much higher exposure to sunlight. The use of Composition Wheels to illustrate differences in sources and processing is shown on the bottom panel, comparing DOM from an organic-rich source with longer exposure to sunlight (A-B-C) versus the same DOM with less sunlight exposure and greater microbial degradation (A-b-c).

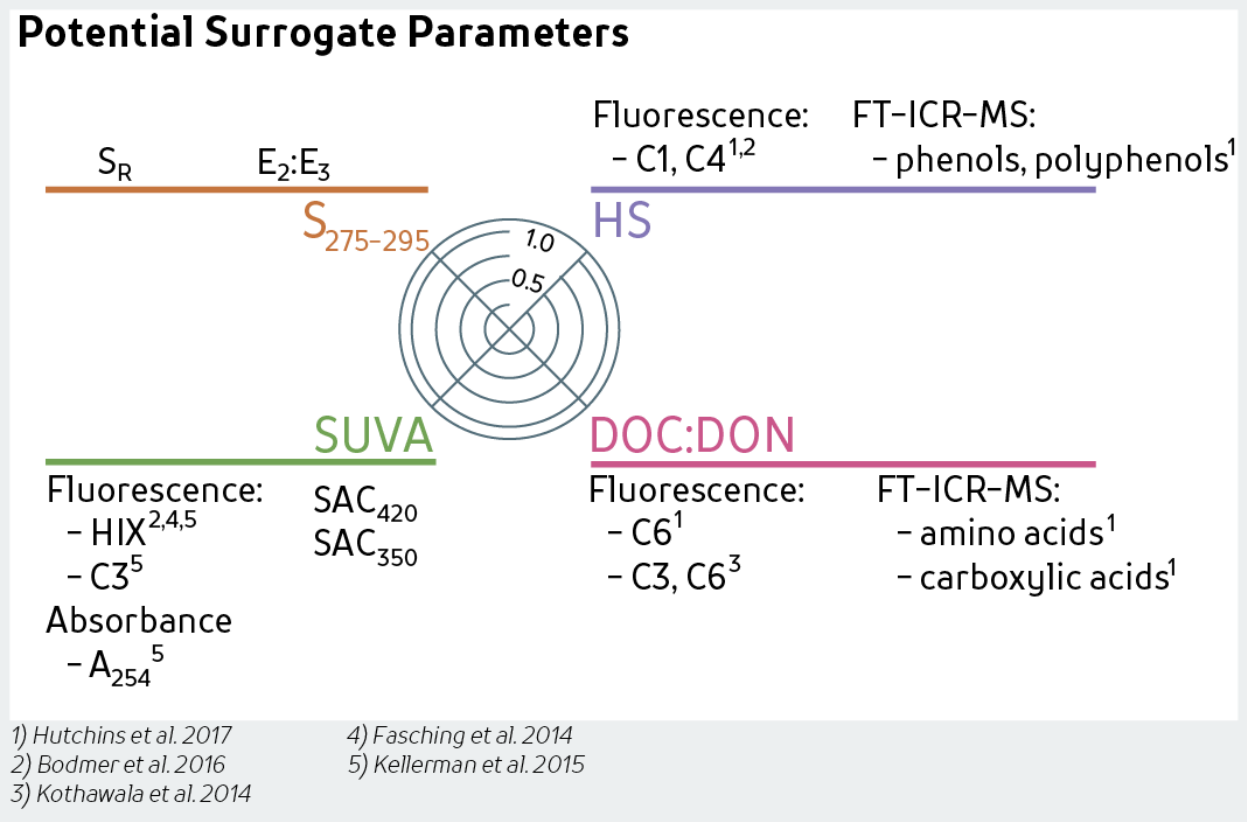

Fig 7. Surrogate parameters for the DOM Composition Wheel.

Supporting information

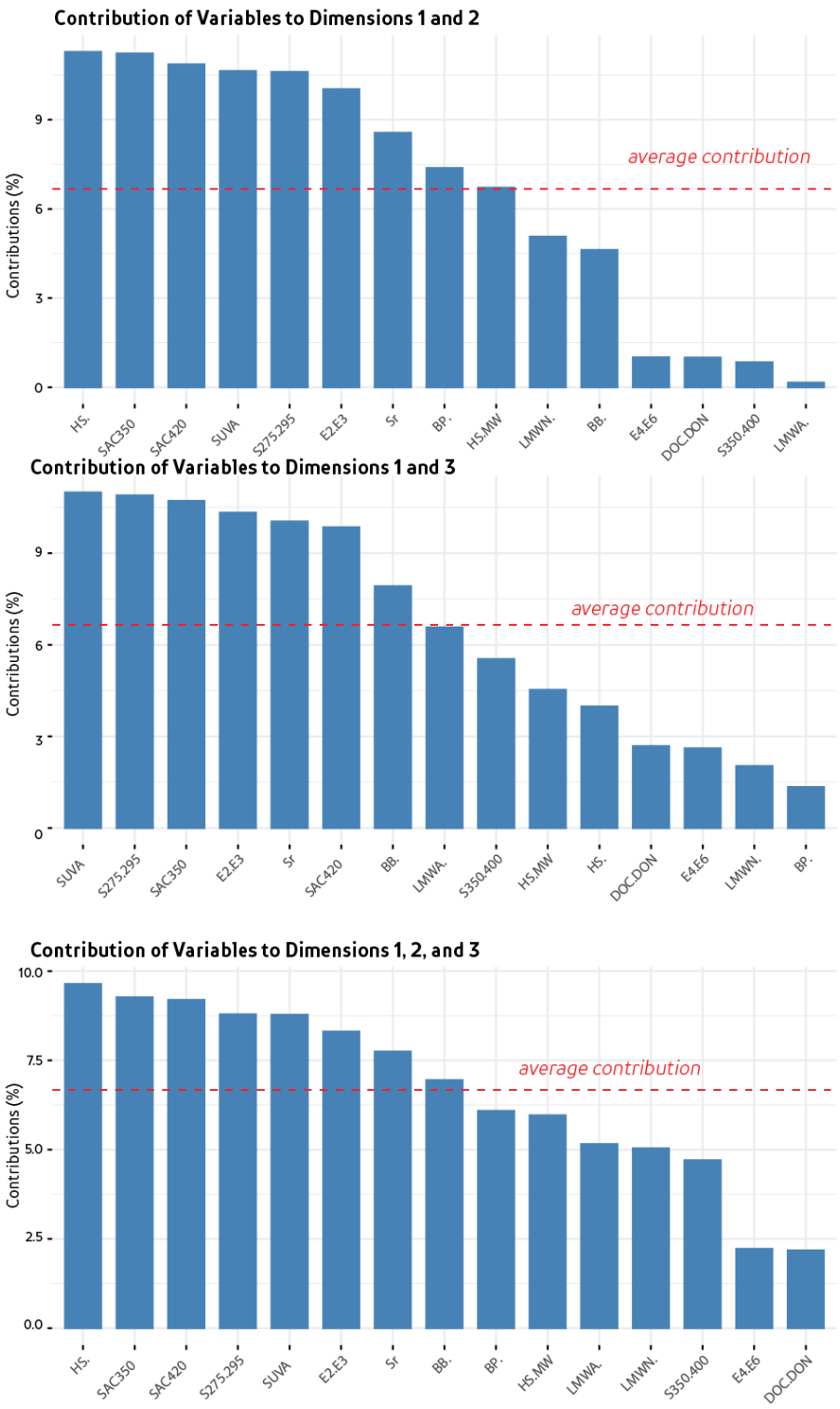

S1 Fig. Contribution of each variable within the PCA.

S1 Table. Environmental description for all sampling sites. Included are the number of total samples taken for DOM concentration with at least one compositional measure (n_{DOC}), and number of samples used from that site in the PCA analysis (n_{PCA}).

SURFACE WATERS				
Name	**Location**	**n_{DOC}**	**n_{PCA}**	**Description**
IISD-Experimental Lakes Area, ON (ELA)	49° 39' 40"N, 93° 43' 48"W Ontario, Canada	**74**	**45**	Boreal forest, underlain by Precambrian bedrock with discontinuous surficial layer of sandy-gravel till. Sampled from 2010 to 2012. Ecozone mean annual temperature: 0.7 C; Ecozone total annual precipitation: 825 mm.
Lakes		*49*	*36*	
Creeks		*25*	*9*	
Grand River, ON (GR)	43° 30' 41"N, 80° 29' 43"W Ontario, Canada	**39**	**-**	Surrounding land predominately agricultural and flows past six wastewater treatment plants. Sampled from 6 consecutive locations along a 90km stretch every two months from 2011 to 2012. Ecozone mean annual temperature: 6.5 C; Ecozone total annual precipitation: 940 mm.
Yellowknife, NT (YK)	62° 27' 14"N, 114° 22' 18"W Northwest Territories, Canada	**23**	**20**	Samples from the Taiga Shield underlain by discontinuous permafrost. Surface waters are surrounded by bedrock and peat plateaux around Yellowknife. Sampled in July or October between 2013 and 2017. Ecozone mean annual temperature: -4.8 C; Ecozone total annual precipitation: 565 mm.
Lakes		*2*	*2*	
Ponds		*8*	*7*	
Rivers		*10*	*9*	
Creek		*3*	*2*	
Mackenzie River, NT (MK)	63° 14' 17"N, 123° 34' 0"W Northwest Territories, Canada	**13**	**-**	Samples taken by the Community Based Monitoring network along the Mackenzie River in July and August of 2015. Samples ranged from WHERE to Inuvik. River flows through Taiga Shield and Taiga Plains.
Rivers		*13*	-	
Wekweètì, NT (WK)	64° 11' 24"N, 114° 11' 10"W Northwest Territories, Canada	**11**	**11**	Situated in the Taiga Shield, below treeline, continuous permafrost. Samples taken in October of 2015 and 2016. Ecozone mean annual temperature: -4.8 C; Ecozone total annual precipitation: 565 mm.
Lakes		*9*	*9*	
Creeks		*2*	*2*	
Daring Lake, NT (DL)	64° 31' 29"N, 111° 40' 24"W Northwest Territories, Canada	**19**	**19**	Found in the Southern Arctic above treeline, continuous permafrost. Ecozone mean annual temperature: -9.8 C; Ecozone total annual precipitation: 313 mm.
Lakes		*7*	*7*	
Ponds		*1*	*1*	
Creeks		*11*	*11*	
Lake Hazen, NU (LH)	81° 49' 30"N, 71° 19' 26"W Nunavut, Canada	**160**	**12**	Tundra located in the high arctic; Lake Hazen Watershed is considered a local polar oasis.
Lakes		*38*	*2*	
Ponds		*18*	*4*	
Creeks		*41*	*1*	
Rivers		*32*	*0*	
Seeps		*31*	*5*	

GROUND WATERS				
Name	**Location**	**n**	**nPCA**	**Description**
Turkey Lakes Watershed, ON (TLW)	47° 2' 54"N, 84° 24' 25"W Ontario, Canada	**16**	**-**	Relatively un-impacted watershed in the Great Lakes-St. Lawrence forest region. Area consists of Precambrian bedrock and surficial glacial deposits of glaciofluvial outwash. Samples collected from depths ranging between 0.90 -

				6.89m below surface. Ecozone mean annual temperature: 0.7 C; Ecozone total annual precipitation: 825 mm.
IISD-Experimental Lakes Area, ON (ELA)	49° 39’ 40”N, 93° 43’ 48”W Ontario, Canada	**17**	**-**	Piezometers constructed in transect along a wetland, ranging from 0.70 - 3.85m below surface. Ecozone mean annual temperature: 0.7 C; Ecozone total annual precipitation: 825 mm.
Nottawasaga Aquifer, ON (NW)	44° 7’ 26”N, 79° 49’ 12”W Ontario, Canada	**6**	**-**	Surficial deposits of glaciolacustrine deposits in an agriculturally-impacted aquifer. Samples collected from single multi-level piezometer within an unconfined surficial sand aquifer at depths of 4.35m, 5.13m, 6.68m, 9.90m, and 11.3m below surface. Ecozone mean annual temperature: 6.5 C; Ecozone total annual precipitation: 940 mm.
Black Brook Watershed, NB (BBK)	47° 6’ 11”N, 67° 45’ 40”W New Brunswick, Canada	**15**	**-**	Site is an agriculturally-impacted aquifer, sampled during the summer of 2012. Surficial deposits of till and small deposits of glacial outwash. Samples taken from twelve domestic wells and three multi-level piezometers (6.1 - 30m below surface). Ecozone mean annual temperature: 4.6 C; Ecozone total annual precipitation: 1185 mm.
Long Point, ON (LP)	42° 34’ 46”N, 80° 22’ 57”W Ontario, Canada	**23**	**-**	Unconfined sand aquifer atop of a clay aquitard. Piezometers range from 1 to 4m below surface. Sampling of groundwater containing a septic plume.
Yellowknife, NT (YK)	62° 27’ 14”N, 114° 22’ 18”W Northwest Territories, Canada	**33**	**16**	Samples from the Taiga Shield underlain by discontinuous permafrost. Surface waters are surrounded by bedrock and peat plateaux around Yellowknife. Sampled in July or October between 2013 and 2017. Ecozone total annual precipitation: 565 mm.
Wekweètì, NT (WK)	64° 11’ 24”N, 114° 11’ 10”W Northwest Territories, Canada	**1**	**1**	Situated in the Taiga Shield, below treeline, continuous permafrost. Samples taken in October of 2015 and 2016. Ecozone total annual precipitation: 565 mm.
Daring Lake, NT (DL)	64° 31’ 29”N, 111° 40’ 24”W Northwest Territories, Canada	**4**	**4**	Found in the Southern Arctic above treeline, continuous permafrost. Ecozone mean annual temperature: -9.8 C; Ecozone total annual precipitation: 313 mm.
Lake Hazen, NU (LH)	81° 49’ 30”N, 71° 19’ 26”W Nunavut, Canada	**17**	**2**	Samples taken from piezometer installed at deepest extent of active-layer (~0.25m). Location was in a subcatchment wetland containing organic-rich soil. Flow direction was through wetland into nearby lake. Organic-rich layer underlain by silt or clay material.

S2 Table. DOM Composition versus Concentration Statistics. Results from a linear model of dissolved organic matter (DOM) composition (SUVA, slope between 275-295nm, DOC:DON,

and humic substances fraction) as predicted by the overall DOM concentration (mg C/L; log transformed).

Parameter	**Linear Regression to log(DOM)**	
	R^2	p-value
SUVA	0.10	<0.01
S275	0.01	0.61
DOC:DON	0.33	<0.01
HSF	0.09	<0.01